Acta Crystallographica Section F
Structural Biology and Crystallization Communications
ISSN 1744-3091

Crystallization and preliminary crystallographic studies of the YafN–YafO complex from *Escherichia coli*

Fan Zhang,[a,b] Li Xing,[a,b] Maikun Teng[a,b]* and Xu Li[a,b]*

[a]School of Life Sciences, University of Science and Technology of China, 96 Jinzhai Road, Hefei, Anhui 230026, People's Republic of China, and [b]Key Laboratory of Structural Biology, Chinese Academy of Sciences, 96 Jinzhai Road, Hefei, Anhui 230026, People's Republic of China

Correspondence e-mail: mkteng@ustc.edu.cn, sachem@ustc.edu.cn

Received 13 February 2012
Accepted 25 May 2012

The ribosome-dependent mRNA interferase YafO from *Escherichia coli* belongs to a type II toxin–antitoxin (TA) system and its cognate antitoxin YafN neutralizes cell toxicity by forming a stable YafN–YafO complex. The YafN–YafO TA system is upregulated by the SOS response (a global response to DNA damage in which the cell cycle is arrested and mutagenesis is induced) and may then inhibit protein synthesis by endoribonuclease activity of YafO with the 50S ribosome subunit. Structural information on the YafN–YafO complex and related complexes would be helpful in order to understand the structural basis of the mechanism of mRNA recognition and cleavage, and the assembly of these complexes. Here, the YafN–YafO complex was expressed and crystallized. Crystals grown by the hanging-drop vapour-diffusion method diffracted to 3.50 Å resolution and belonged to the hexagonal space group *P*622, with unit-cell parameters $a = 86.14$, $b = 86.14$, $c = 173.11$ Å, $\alpha = \beta = 90$, $\gamma = 120^\circ$. Both Matthews coefficient analysis and the self-rotation function suggested the presence of one molecule per asymmetric unit in the crystal, with a solvent content of 65.69% ($V_M = 3.58$ Å^3 Da^{-1}).

1. Introduction

Almost all free-living bacteria contain a number of toxin–antitoxin (TA) operons, the toxin products of which cause cell-growth arrest and eventual cell death (Yamaguchi & Inouye, 2011). These TA systems are classified into three groups (types I, II and III) on the basis of the function of the antitoxin. Type I TA systems consist of an RNA antitoxin and a protein toxin, in which the RNA antitoxin inhibits the translation of the toxin mRNA (Gerdes & Wagner, 2007). Type II TA systems typically consist of two genes in an operon that are transcriptionally and translationally coupled, in which the upstream gene usually encodes a labile antitoxin protein and the downstream gene usually encodes a stable toxin protein (Shao *et al.*, 2011). Type III TA systems, which were recently identified in *Pectobacterium atrosepticum*, rely on direct interaction between a toxin protein and an RNA antitoxin. The toxic effects of the protein are neutralized by the RNA antitoxin (Fineran *et al.*, 2009).

In *Escherichia coli*, there are eight well characterized TA systems: MazF–MazE, RelE–RelB, ChpBK–ChpBI (also known as ChpB–ChpS), YafQ–DinJ, YoeB–YefM, HipA–HipB, YafO–YafN and MqsR–MqsA (Yamaguchi & Inouye, 2011). In addition, bioinformatics and biochemical analyses have identified 28 putative TA systems encoded by the *E. coli* K-12 genome (Sevin & Barloy-Hubler, 2007). The cellular targets of these TA-system toxin products are highly diverse and expression of these toxins seems to be induced under different stress conditions, suggesting that the toxins play diverse roles in the cell.

One of the TA-system toxins, YafO, is encoded by the *yafO* gene, which lies downstream of *dinB* and *yafN* in the *dinB-yafN-yafO-yafP* operon (McKenzie *et al.*, 2003). Under ultraviolet irradiation, the transcription level of YafO increases fourfold, suggesting that YafO may be involved in an SOS reaction triggered by the DNA damage response (Courcelle *et al.*, 2001). In this type II TA system, the toxin YafO and its cognate antitoxin YafN form a stable TA complex which blocks toxin function. As the antitoxin YafN is less stable than the toxin YafO in the cell, it has to be constantly produced to inhibit

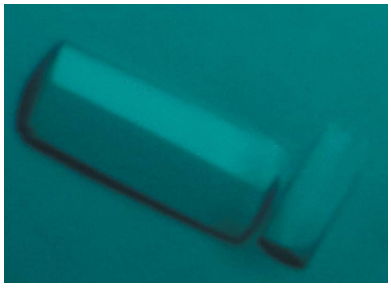

the toxin (Yamaguchi & Inouye, 2009). Although *yafNO* is co-transcribed with *dinB*, a gene that underlies stress-induced mutagenesis mechanisms in *E. coli* and encodes DNA polymerase IV, the TA system is not required for stress-induced mutagenesis. Additionally, *yafP*, which encodes a protein of unknown function, lies downstream in the operon (Singletary *et al.*, 2009).

Under stress conditions, YafN may be digested by stress-induced proteases to release free YafO, resulting in the inhibition of protein synthesis. In the absence of ribosome, YafO alone does not function to inhibit protein synthesis. However, when YafO associates with the 50S subunit of the 70S ribosome its latent endoribonuclease activity is induced and it may then effectively inhibit protein synthesis by cleaving mRNAs 11–13 bases downstream of the initiation codon. Thus, YafO is also termed as a ribosome-dependent mRNA interferase that inhibits protein synthesis but not DNA or RNA synthesis (Zhang *et al.*, 2009).

Dissection of the interactions of YafO with its intracellular targets (the 50S ribosome subunit and mRNAs) and elucidation of the tertiary structure of the YafN–YafO complex may provide exciting insights into antitoxin–toxin behaviour, which would be helpful for understanding the structural basis of mRNA recognition and cleavage by the ribosome-dependent mRNA interferase YafO and the mechanism of neutralization of toxicity by the antitoxin YafN.

2. Materials and methods

2.1. Cloning and expression

Primers of sense strand 5′-GGCGCGCATATGCATCGAATTC-TCGCTGA-3′ and antisense strand 5′-CCCGGTCGACAAAAC-GCATGCGAAACGCTTC-3′ (Invitrogen) were used to amplify the *yafN-yafO* antitoxin–toxin operon gene by polymerase chain reaction (PCR) from genomic DNA isolated from *E. coli* strain K-12. The PCR product was digested by restriction endonucleases *Nde*I and *Xho*I and then ligated into pET-22b vector (Novagen) with a hexahistidine tag (LEHHHHHH) at the C-terminus of YafO; no additional non-natural amino acids were added to the *yafN* gene product. After sequencing, the plasmid was transformed into *E. coli* Rosetta 2 competent cells (Novagen). The transformant was grown in 1.6 l Luria–Bertani (LB) medium containing 100 µg ml^{-1} ampicillin at 310 K. When an OD_{600} of 0.6–0.8 was reached, 0.5 m*M* isopropyl *β*-D-1-thiogalactopyranoside (IPTG) was added for induction. After 5 h induction at 310 K, the cells were harvested by centrifugation at 6000*g* for 10 min.

2.2. Purification

The harvested cells were suspended in buffer *A* (50 m*M* Tris–HCl pH 8.5, 500 m*M* NaCl) and lysed by sonification on ice. The cell lysate was centrifuged and the pellets were denaturated with buffer *B* (50 m*M* Tris–HCl pH 8.5, 500 m*M* NaCl, 8 *M* urea) for more than 10 h at 277 K. The denaturated solution was centrifuged again and the clear supernatant was passed through an Ni–NTA column (Qiagen) previously equilibrated with buffer *B*. Refolding of the bound complex was performed using a linear 8–0 *M* urea gradient starting with buffer *B*. Unbound proteins were washed away with buffer *A* containing 50 m*M* imidazole. The bound protein was eluted with buffer *A* containing 500 m*M* imidazole. After ultrafiltration to 2 ml using a Millipore 10 kDa centrifugal device, the target protein was purified using a Superdex 200 (GE Healthcare) gel-filtration chromatography column previously equilibrated with buffer *A*. Fractions containing the recombinant complex were determined by SDS–PAGE.

The identity of the proteins was further confirmed by LC-MS/MS peptide-mapping experiments. Briefly, different bands from the SDS–PAGE were in-gel digested with trypsin and the digested peptides were chromatographically separated (Jupiter 5 µm C18 300A; Phenomenex Inc.) using a Surveyor system (Thermo Fisher Scientific, California, USA) connected to an LTQ mass spectrometer (Thermo Fisher Scientific). The chromatographic method used a flow rate of 90 nl min^{-1} with a step gradient from mobile phase *A* containing 0.1% formic acid in water to mobile phase *B* containing 0.1% formic acid in acetonitrile. MS/MS fragmentation was performed using collision-induced dissociation (CID) with an activation *Q* of 0.250, an activation time of 30.0 ms, 35% of normalized collision energy and an isolation width of 1.0 Da. MS/MS data were compared using *SEQUEST* software (Thermo Fisher Scientific).

2.3. Crystallization

The recombinant YafN–YafO complex was concentrated to 20 mg ml^{-1} (as calculated from the OD_{280} using a molar absorption coefficient of 19 940 M^{-1} cm^{-1}; Eppendorf BioPhotometer Plus) by centrifugal ultrafiltration (Millipore; 10 kDa cutoff) prior to crystallization trials. The hexahistidine tag of YafO was not removed before crystallization. Crystallization screening of the YafN–YafO complex was performed with a Mosquito liquid-handling robot (TTP LabTech) using the vapour-diffusion method in 96-well crystallization plates at 289 K. Drops were prepared by mixing 0.25 µl protein solution at 20 mg ml^{-1} protein with 0.25 µl reservoir solution and were equilibrated against 100 µl reservoir solution using 672 different conditions based on Crystal Screen, Crystal Screen 2, Index, SaltRx, Grid1, Grid2, Complex and Complex pH crystallization screens from Hampton Research and Molecular Dimensions. After 3 d, the best crystals were observed in drops consisting of 12%(*w*/*v*) ethanol, 4%(*w*/*v*) polyethylene glycol 400, 0.1 *M* sodium acetate pH 4.6. Subsequent screening was performed by varying the pH and the polyethylene glycol 400 concentration. Drops were prepared by mixing 1 µl protein solution at 15 mg ml^{-1} with 1 µl reservoir solution and were equilibrated against 200 µl reservoir solution in 24-well crystallization plates at 289 K. The optimized crystals appeared in drops consisting of 12%(*w*/*v*) ethanol, 3%(*w*/*v*) polyethylene glycol 400, 0.1 *M* sodium acetate pH 4.8.

2.4. Data collection and processing

A crystal mounted in a loop was briefly soaked in a cryoprotectant solution consisting of the corresponding reservoir solution supplemented with 25%(*v*/*v*) glycerol and flash-cooled in liquid nitrogen. X-ray diffraction data were collected on beamline 17U1 at Shanghai Synchrotron Radiation Facility (SSRF) using a Jupiter CCD detector. All frames were collected at 100 K using a 1° oscillation angle and an exposure time of 1 s per frame. The crystal-to-detector distance was set to 400 mm. The complete diffraction data set was processed using *HKL*-2000 (Otwinowski & Minor, 1997).

3. Results and discussion

In the expression strain, the recombinant YafN and YafO proteins were expressed as two independent polypeptides which were both distributed into inclusion bodies; the expression level of YafN was much greater than that of YafO. To purify these two proteins from the inclusion bodies, a denaturing and refolding method was used. During the refolding process on the Ni–NTA column, a large proportion of the YafN protein was eluted by the refolding buffer. Although only YafO carried a His tag, a small proportion of YafN was

eluted with abundant YafO when the protein bound to the Ni–NTA column was eluted with buffer *A* containing 500 m*M* imidazole. After gel-filtration chromatography using a Superdex 200 column, YafN–YafO and YafO–YafO complexes both existed in the sample (Fig. 1, lanes 1 and 2). The ∼27 kDa band was determined to be the YafN–YafO complex: 65 amino acids of YafO covering 49.24% of the 132-amino-acid sequence and 40 amino acids of YafN covering 41.24% of the 97-amino-acid sequence were identified. The ∼30 kDa band was determined to be the YafO dimer: 65 amino acids of YafO covering 49.24% of the 132-amino-acid sequence were identified.

Rod-like crystals of the YafN–YafO complex were obtained using an optimized precipitant condition consisting of 12%(*w*/*v*) ethanol, 3%(*w*/*v*) polyethylene glycol 400, 0.1 *M* sodium acetate pH 4.8 (Fig. 2). A total of 180 diffraction images were recorded from a single crystal. The YafN–YafO complex crystal diffracted to a maximum resolution of 3.50 Å and belonged to the hexagonal space group *P*622, with unit-cell parameters a = 86.14, b = 86.14, c = 173.11 Å, $\alpha = \beta = 90$, $\gamma = 120^\circ$. The number of molecules in the asymmetric unit was assumed to be one based on the Matthews coefficient (3.58 Å^3 Da^{-1}), with a solvent content of 65.69%. Detailed data-processing statistics are given in Table 1.

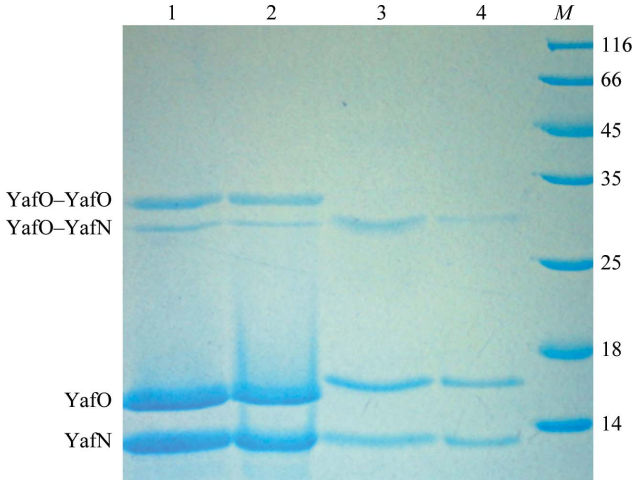

Figure 1
SDS–PAGE analysis of the YafN–YafO complex before and after crystallization. The protein was analyzed on 15% SDS–PAGE and stained with Coomassie Blue. Lane 1, nonreducing SDS–PAGE of the purified YafN–YafO complex; lane 2, reducing SDS–PAGE of the purified YafN–YafO complex; lane 3, nonreducing SDS–PAGE of redissolved crystals of the YafN–YafO complex; lane 4, reducing SDS–PAGE of redissolved crystals of the YafN–YafO complex. Lane *M*, molecular-mass marker (labelled in kDa).

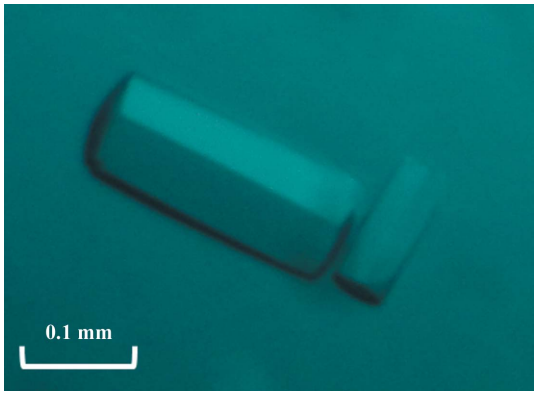

Figure 2
Crystals of the YafN–YafO complex grown using 0.1 *M* sodium acetate pH 4.8, 12% ethanol, 3% polyethylene glycol 400.

Table 1
Data-collection statistics for the YafN–YafO complex.

Values in parentheses are for the highest resolution shell.

Space group	*P*622
Wavelength (Å)	0.9784
Unit-cell parameters (Å, °)	a = 86.14, b = 86.14, c = 173.11, $\alpha = \beta = 90$, $\gamma = 120$
Resolution limits (Å)	50.00–3.50 (3.56–3.50)
No. of observed reflections	45495
No. of unique reflections	5205
Completeness (%)	99.0 (99.6)
$R_{\rm p.i.m.}$† (%)	3.3 (16.5)
$R_{\rm meas}$‡ (%)	10.4 (53.9)
$R_{\rm merge}$§ (%)	8.1 (55.6)
Mean $I/\sigma(I)$	30.9 (5.5)
$V_{\rm M}$ (Å^3 Da^{-1})	3.58
No. of subunits per asymmetric unit	1
Solvent content (%)	65.69

† $R_{\rm p.i.m.} = \sum_{hkl}\{1/[N(hkl)-1]\}^{1/2}\sum_i |I_i(hkl) - \langle I(hkl)\rangle|/\sum_{hkl}\sum_i I_i(hkl)$, where $I_i(hkl)$ is the ith observation of reflection hkl, $\langle I(hkl)\rangle$ is the weighted average intensity of all observations i of reflection hkl and $N(hkl)$ is the multiplicity. ‡ $R_{\rm meas} = \sum_{hkl}\{N(hkl)/[N(hkl)-1]\}^{1/2}\sum_i |I_i(hkl) - \langle I(hkl)\rangle|/\sum_{hkl}\sum_i I_i(hkl)$, where $I_i(hkl)$ is the ith observation of reflection hkl, $\langle I(hkl)\rangle$ is the weighted average intensity of all observations i of reflection hkl and $N(hkl)$ is the multiplicity. § $R_{\rm merge} = \sum_{hkl}\sum_i |I_i(hkl) - \langle I(hkl)\rangle|/\sum_{hkl}\sum_i I_i(hkl)$, where $I_i(hkl)$ is the ith observation of reflection hkl and $\langle I(hkl)\rangle$ is the weighted average intensity of all observations i of reflection hkl.

To verify the composition of our crystal, crystals were washed twice with reservoir solution and redissolved. The redissolved solution was analyzed by SDS–PAGE under both reducing and nonreducing conditions (Fig. 1, lanes 3 and 4). The ∼27 kDa band was determined to be the YafN–YafO complex: 65 amino acids of YafO covering 49.24% of the 132-amino-acid sequence and 40 amino acids of YafN covering 41.24% of the 97-amino-acid sequence were identified. The ∼15 kDa band was determined to be YafO protein: 84 amino acids of YafO covering 63.64% of the 132-amino-acid sequence were identified. The ∼12 kDa band was determined to be YafN protein: 50 amino acids of YafN covering 51.55% of the 97-amino-acid sequence were identified.

It was difficult to directly determine the structure of the YafN–YafO complex by the molecular-replacement method. Experimental phasing was carried out using the single-wavelength anomalous dispersion (SAD) method. Crystals of SeMet-substituted protein were grown using the same conditions as were used for the native YafN–YafO complex.

We are grateful to the staff members at SSRF for the collection of diffraction data. Financial support for this project was provided by the Fundamental Research Funds for the Central Universities, the Chinese National Natural Science Foundation (grant Nos. 31130018, 30900224 and 10979039), the Chinese Ministry of Science and Technology (grant Nos. 2012CB917200 and 2009CB825500), the Science and Technological Fund of Anhui Province for Outstanding Youth (grant No. 10040606Y11), the Anhui Provincial Natural Science Foundation (grant No. 090413081) and the Education Department of Anhui Province (grant No. 2009SQRZ007ZD).

References

Courcelle, J., Khodursky, A., Peter, B., Brown, P. O. & Hanawalt, P. C. (2001). *Genetics*, **158**, 41–64.
Fineran, P. C., Blower, T. R., Foulds, I. J., Humphreys, D. P., Lilley, K. S. & Salmond, G. P. (2009). *Proc. Natl Acad. Sci. USA*, **106**, 894–899.
Gerdes, K. & Wagner, E. G. (2007). *Curr. Opin. Microbiol.* **10**, 117–124.

McKenzie, G. J., Magner, D. B., Lee, P. L. & Rosenberg, S. M. (2003). *J. Bacteriol.* **185**, 3972–3977.
Otwinowski, Z. & Minor, W. (1997). *Methods Enzymol.* **276**, 307–326.
Sevin, E. W. & Barloy-Hubler, F. (2007). *Genome Biol.* **8**, R155.
Shao, Y., Harrison, E. M., Bi, D., Tai, C., He, X., Ou, H.-Y., Rajakumar, K. & Deng, Z. (2011). *Nucleic Acids Res.* **39**, D606–D611.
Singletary, L. A., Gibson, J. L., Tanner, E. J., McKenzie, G. J., Lee, P. L., Gonzalez, C. & Rosenberg, S. M. (2009). *J. Bacteriol.* **191**, 7456–7465.
Yamaguchi, Y. & Inouye, M. (2009). *Prog. Mol. Biol. Transl. Sci.* **85**, 467–500.
Yamaguchi, Y. & Inouye, M. (2011). *Nature Rev. Microbiol.* **9**, 779–790.
Zhang, Y., Yamaguchi, Y. & Inouye, M. (2009). *J. Biol. Chem.* **284**, 25522–25531.